# II.E.7 Photoelectrochemical Hydrogen Production Using New Combinatorial Chemistry Derived Materials

Eric W. McFarland (Primary Contact),
Yong-Sheng Hu, Alan Kleiman-Shwarsctein,
Peng Zhang, and Arnold J. Forman
University of California
Dept. of Chemical Engineering
Santa Barbara, CA 93106-5080
Phone: (805) 893-4343; Fax: (805) 893-4731
E-mail: mcfar@engineering.ucsb.edu

DOE Technology Development Manager:
Roxanne Garland
Phone: (202) 586-7260; Fax: (202) 586-2373
E-mail: Roxanne.Garland@ee.doe.gov

DOE Project Officer: David Peterson
Phone: (303) 275-4956; Fax: (303) 275-4788
E-mail: David.Peterson@go.doe.gov

Contract Number: DE-FG36-05GO15040

Start Date: September 1, 2004
Projected End Date: December 31, 2009

## Objectives

- Continue synthesis and screening of libraries designed in previous years and follow promising (lead) materials as they are identified.
- Perform exploratory design, synthesis and screening of new mixed metal-oxides based on solid solutions and substitutional doping of Zn, W, Ti, Cu and Fe host oxides with the aim of improving the absorption of visible light to an equivalent of a material with a bandgap of approximately 1.8-2.3 eV.
- Explore synthesis parameters and post-processing surface modification to optimize conductivity, tune the bandgap position and minimize charge trapping and surface recombination of materials selected from Objectives 1-2.
- Investigate metal/metal oxide libraries for electrocatalytic hydrogen production and expand our high-throughput screening to include electrocatalytic overpotential as a routine screen.
- Continue synthesis of libraries of semiconductor heterostructures for improved charge separation efficiency and/or stability by creating libraries where heterojunctions will be formed both for passivating, otherwise unstable, material surfaces (e.g. wide gap oxide on narrow gap material) as well as for utilizing two-photon tandem absorption processes.
- Explore the theoretical and practical economic potential of alternative surface redox reactions.
- Development of iron oxide thin films based on electrodeposition and self assembly methods.

## Technical Barriers

This project addresses the following technical barriers from the Hydrogen Production section of the Hydrogen. Fuel Cells and Infrastructure Technologies Program Multi-Year Research, Development and Demonstration Plan:

(Y) Materials Efficiency
(Z) Materials Durability
(AA) PEC Device and System Auxiliary Material
(AB) Bulk Materials Synthesis

## Technical Targets

| Characteristics | Units | 2003 Target | 2006 Target | Achieved 2007 | 2013 Target |
|---|---|---|---|---|---|
| Usable semiconductor bandgap | eV | 2.8 | 2.8 | 2.1 | 2.3 |
| Chemical conversion process efficiency (EC) | % | 4 | 4 | 1 | 10 |
| Plant solar-to-hydrogen efficiency (STH) | % | NA | NA | NA | 8 |
| Plant durability | hr | NA | NA | <100 | 1,000 |

NA - not applicable

## Approach

- Systems development
  - Continuing synthesis and high-throughput screening system upgrades:
    - More samples/higher throughput
    - Faster measurements
    - Increased reproducibility
  - Develop an automated electrochemical synthesis system.
  - Develop chemistry for iron oxide nanorods growth (self assembly).

  - Develop a single slurry reactor for measuring internal quantum efficiency (IQE) from colloidal photocatalysts.
- Combinatorial library synthesis and screening
  - Using new and existing high-throughput synthesis and screening technology, create and screen suitable new mixed oxide materials for electrochemical/photoelectrochemical (PEC) hydrogen production.
  - Catalyze the surfaces and engineer/modify the band-edges of the identified semiconductor materials as required.
  - Synthesize, using conventional routes, iron oxide based materials in libraries by electrodeposition and self assembly of nanorods for detailed structure and property analysis.
  - Determine if existing photovoltaic device structures could be easily modified to effect the direct splitting of water.

## Accomplishments

- Developed an automated electrochemical synthesis system.
- Developed a second generation automated system for photoelectrochemical (photocurrent, photovoltage, flat-band potential, incident photon conversion efficiency [IPCE]) characterization.
- Explored the synthesis of iron oxide-based system by electrodeposition.
- Development of synthesis conditions for the synthesis of iron oxide nanorods with control over the feature size of the nanorods.
- Explored the synthesis of mesoporous iron oxide by a template method.

✧ ✧ ✧ ✧ ✧

## Introduction

The overall project objective is to discover and optimize an efficient, practical, and economically sustainable material for photoelectrochemical production of bulk hydrogen from water – a clean, renewable route to hydrogen energy. The properties of the semiconductors investigated for this application, which are similar to those in photovoltaic devices, must satisfy conditions in several areas if cost-effective hydrogen production is to be realized: (1) efficient solar absorption, (2) effective charge separation/transport, (3) appropriate conduction band/valence band energies relative to $H_2$ and $O_2$ redox potentials (“band matching”), (4) facile interfacial charge transfer, (5) long-term stability, and (6) low cost. A material which satisfies all the above conditions simultaneously could provide clean hydrogen in bulk and at low cost; unfortunately, no such material or system has been discovered or developed to date. The DOE has identified the following future targets for solar-to-hydrogen efficiency and durability: 2006, 4%; 2013, 8% and 1,000 hrs; 2018, 10% and 5,000 hrs.

Hematite ($\alpha$-$Fe_2O_3$) has many potential advantages for hydrogen photoproduction. It has a bandgap of 2-2.2 eV (absorbs approximately 40% of the solar spectrum), it is stable in electrolytes over a wide range of pHs and is abundant, inexpensive and non toxic [1-3]. To date, several factors have limited the use of this material as an efficient photocatalyst, including poor charge transfer, high recombination rates of photogenerated electrons and holes [4,5] and inappropriate conduction band position which is more positive than the redox level of $H^+/H_2$. The undesirable electrical properties are partially due to the hopping mechanism of charge transfer via oxygen vacancies, grain boundaries, and surface traps, resulting in relatively low quantum yields, while the positive conduction band position is due to the Fe 3d electrons. Efforts have been devoted to reducing the resistance of thin films by increasing the amount of charge carriers or transferring electrons along the (001) planes of the hematite, which has four orders of magnitude lower resistance than transport perpendicular to this plane. Several strategies have been proposed to overcome these limitations by tailoring the hematite structure to allow more efficient transport and collection of photogenerated charge carriers, doping with heteroatoms and loading surface electrocatalysts (e.g. Pt, Au, $RuO_2$). Most work has been devoted to doping the iron oxide with heteroatoms as a means of improving PEC performance [5,6]. Our idea is that by deliberately doping hematite with selected heteroatoms and being able to control the growth dimensions, crystal orientation, facets exposed as well as modifying the surface such limitations may be overcome. There is much diversity to explore in searching for the appropriate combination of dopant species to improve photocatalytic performance [5,8-10] as well as to understand and engineer the crystal structure, orientation and size of the crystalline domains of hematite.

## Approach

The approach of this project involves the application of combinatorial chemistry methods to discover and optimize PEC materials and systems for cost-effective hydrogen production. This represents a shift in the research paradigm from conventional chemical research in a combinatorial approach that features systematic and high-speed exploration of new metal-oxide based solid-state materials. By investigating large arrays of diverse materials, we are working to improve the understanding of the fundamental mechanisms and composition-structure-property relationships within these systems while discovering new and useful energy-producing photocatalysts. It should be also noted that our approach focuses upon the investigation of semiconductor materials that are inherently inexpensive, such as iron oxide. Iron oxide materials can be synthesized by rapid serial electrodeposition techniques or can be synthesized by sol-gel or self assembly of nanorods, however, the limiting step in this case is still the high throughput screening of materials, thus by utilizing the high throughput screening system we can expedite the material discovery.

## Results

We have redesigned our automated electrochemical synthesis system to allow using cyclic voltammogram deposition method for a variety of new materials and we have focused mainly on $Fe_2O_3$ host, investigating libraries of variable composition and structure. A sketch of the high throughput electrochemical synthesis system and computer-controlled user interface are shown in Figure 1. During the synthetic process, electrochemical parameters like voltage range, scan rate, cycle number, etc. can be easily controlled by program. We have also developed a general electrochemical method to synthesize $\alpha$-$Fe_2O_3$ libraries.

$\alpha$-$Fe_2O_3$ thin films have been synthesized by electrochemical cyclic voltammogram deposition techniques. Results show that doping with heteroatoms can be realized by co-electrodeposition. Around 30 dopants such as Al, Zn, Cu, Ni, Co, Cr, Mo, Ti, Pt, etc. were investigated. Doping with Al, Ti, Pt and Mo exhibits the most promising results. Here we take Pt and Mo as examples to describe the structure and PEC performance. Figures 2a, b and c show the scanning electron microscope (SEM) images of undoped Pt- and Mo-doped iron oxide thin films. The change of the morphology before and after doping is due to the changes in the nucleation and growth rates, rather than being induced by sintering during calcination, which decrease the size of the grains in the film. The doped thin films appear more uniform and dense than those of undoped controls. Figure 2d shows the X-ray diffraction (XRD) patterns of the undoped and doped iron oxide thin films. With the exception of the marked substrate peaks, the XRD data are consistent with the rhombohedral symmetry of $Fe_2O_3$ (JCPDS card No. 33-0664) indicating the presence of a crystalline hematite phase and absence of other impurity phases at a level greater than the instrument sensitivity. Raman spectra, Figure 2e, for the undoped, Pt- and Mo-doped iron oxide thin films show peaks ascribed to the $\alpha$-$Fe_2O_3$ crystalline phase. In the case of Pt-doped sample, there is a peak located at 657 $cm^{-1}$ whose intensity is much higher than that of peak located at 604 $cm^{-1}$, which is different from the undoped and Mo-doped samples. At moment, the reason still remains unknown. The distribution of dopant as a function of depth within the films was examined by X-ray photoelectron spectroscopy (XPS) ion etching. Figure 2f presents the XPS etching profile obtained from the films before and after ion etching by $Ar^+$ sputtering. It can be seen that Pt was homogeneously distributed within the film whereas Mo was enriched on the surface.

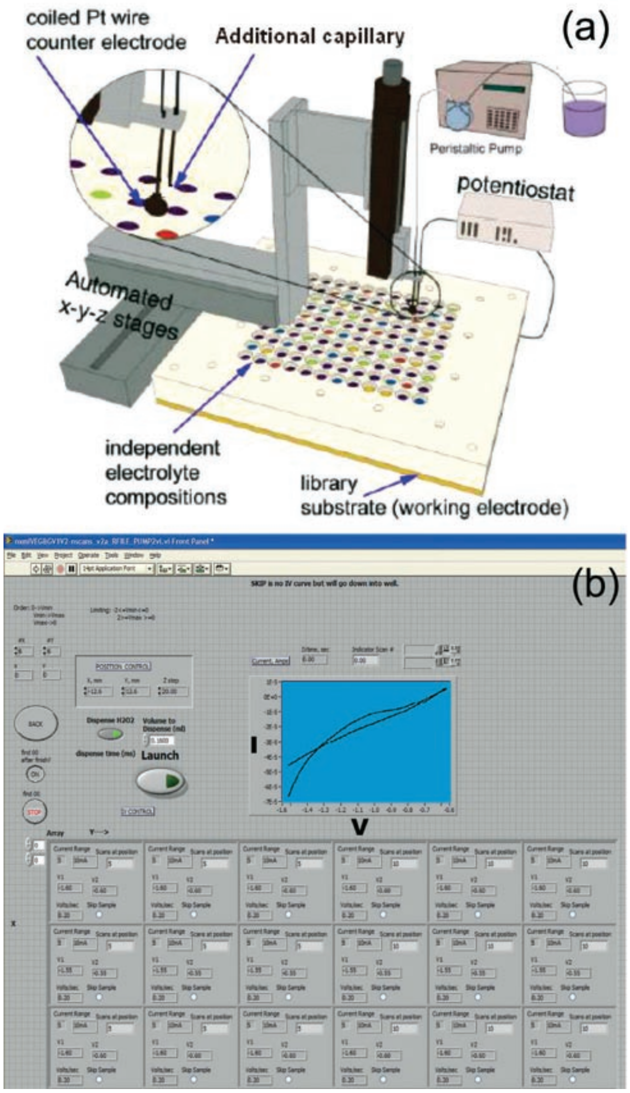

**FIGURE 1.** (a) Automated electrochemical synthesis system based on rapid-serial cyclic voltammogram deposition: 36 independent electrochemical cells are sealed upon a single conductive substrate. (b) User interface programmed based on Labview.

The ultraviolet-visual spectra of the undoped and doped samples on fluorine doped tin oxide substrates obtained in transmission mode are shown in Figure 3a. The spectra were normalized to 700 nm. Very small differences in optical densities of the samples were observed, which might be due to variations in the thickness and morphologically dependent scattering

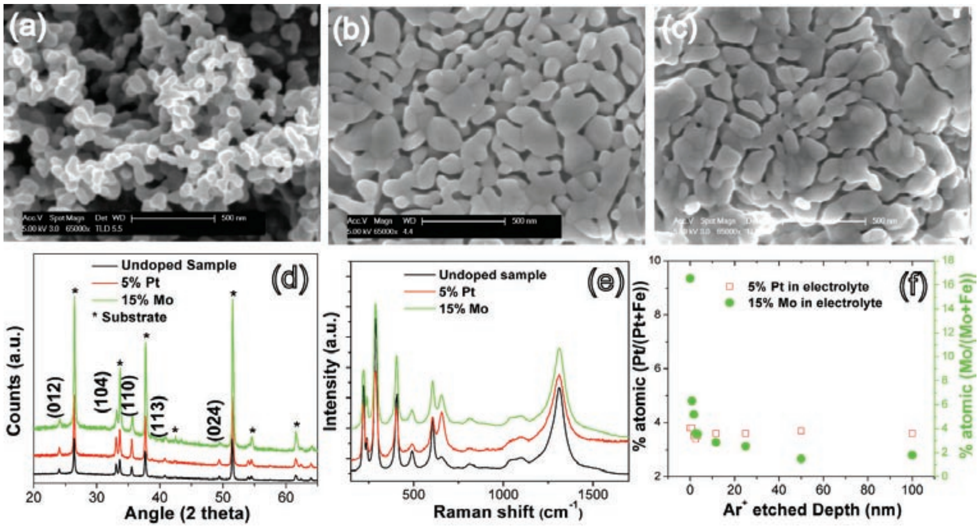

**FIGURE 2.** Structural characterizations. SEM images of undoped iron oxide thin film (a), 5% Pt doped iron oxide thin film (b) and 15% Mo doped iron oxide thin film (c); XRD patterns for undoped, 5% Pt and 15% Mo doped iron oxide thin films (d); Raman spectra for undoped, 5% Pt and 15% Mo doped iron oxide thin films (e); XPS depth profiles for 5% Pt and 15% Mo doped iron oxide thin films.

of the deposited films. The optical bandgap of the samples was calculated from a Tauc Plot (Figure 3a inset), and the best fit was found for the direct bandgap transition rather than an indirect bandgap with values of 2.0 eV for the Pt-doped sample and 2.1 eV for both the undoped and Mo-doped samples. The IPCE as a function of wavelength for the undoped and doped iron oxide thin films at different applied potentials is shown in Figure 3b. The IPCE of the Pt- and Mo-doped sample is significantly greater under all conditions than that of the undoped sample (e.g., at 0.4 V, ~12% vs 3% [400 nm]). In the case of Mo-doped sample, the IPCE values at a lower bias are higher than those of Pt-doped sample. The overall energy efficiency at different wavelengths and applied potentials can be calculated based on the light and electrical energy inputs, Efficiency $= [(1.23 - E_{appl}) \times i_{photocurrent}]/j_{photons}$. For instance, the Pt-doped sample at 400 nm and 0.46 V (vs. 2-electrode system) would yield an overall energy efficiency of ~3%, which is nearly four times higher than that of undoped sample.

Due to the poor charge transfer in iron oxides, nanostructured design is desired in order to reduce the transport length for both electrons and holes. In this viewpoint, we have successfully synthesized worm-hole and ordered mesoporous iron oxides as shown in Figure 4a and b through a template approach. Nano dendrite-like iron oxide thin films were also obtained by a moderate hydrothermal method as shown in Figure 4c. In order to reduce recombination rate of photogenerated electrons and holes and enhance the kinetics of the oxygen evolution reaction, surface passivation and electrocatalysts are required. Such structure was

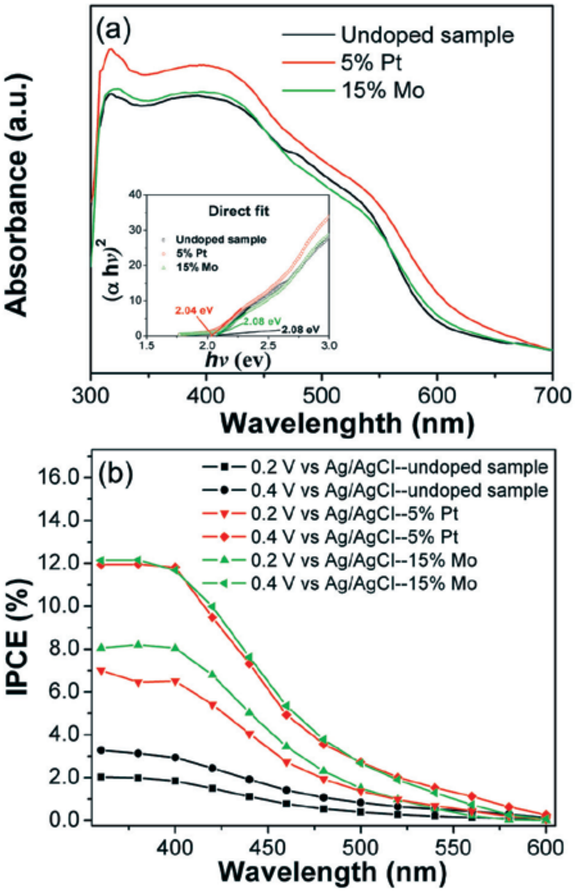

**FIGURE 3.** Optical properties and PEC performance. (a) UV-Visible spectra of undoped, 5% Pt and 15% Mo doped iron oxide thin films, inset showing the Tauc plots; (b) IPCE of the undoped, 5% Pt and 15% Mo doped iron oxide thin films at different applied potentials in $N_2$ degassed 1M NaOH.

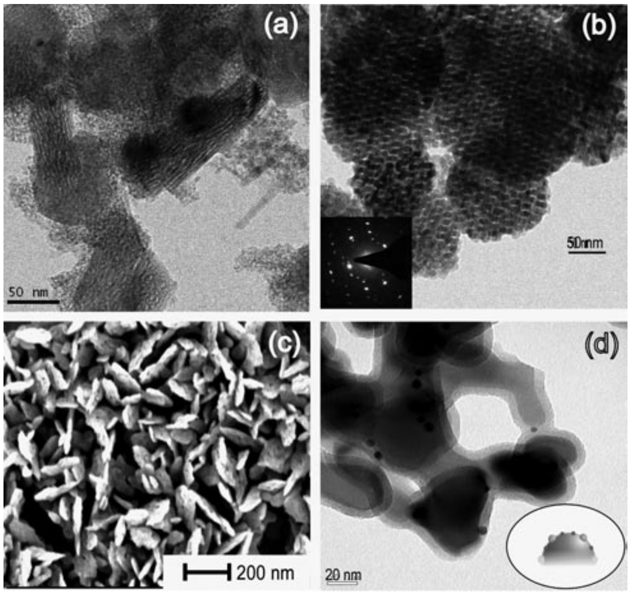

**FIGURE 4.** Nanostructured design of iron oxides. (a) worm-hole mesoporous α-$Fe_2O_3$ prepared by a soft template; (b) ordered mesoporous α-$Fe_2O_3$ prepared by a hard template; (c) dendrite-like α-$Fe_2O_3$ prepared by a hydrotherm method; (d) α-$Fe_2O_3$ nanoparticles with surface modification.

realized by loading Au nanoparticles on the surface of iron oxide particles coated with an ultra-thin layer of $SiO_2$ as shown in Figure 4d. It can be expected that these unique nanostructured iron oxides would show improved photocatalytic performance whose results will be reported in the next annual report.

## Conclusions and Future Directions

- The methodology of combinatorial material science has been applied to expedite the discovery of improved photocatalytic materials for hydrogen production.
- The automatic electrochemical system can be used to reliably synthesize iron oxide thin films doped with various heteroatoms.
- The best performing electrodeposited iron oxide samples are those doped with Al, Ti, Mo and Pt atoms. The Pt- and Mo-doped iron oxide thin films show a remarkable improvement in efficiency for photoelectrochemical water splitting compared to undoped samples. Further work on understanding the doping effect on the mechanism and PEC behavior is ongoing.
- Various desired nanostructured iron oxide materials have been synthesized with variation on the particle size, porosity, and surface area as well as surface modification.
- Continue optimization of doped hematite: theory guided, multi-atom substitutions of α-$Fe_2O_3$, especially on both a donor and an acceptor co-doping.
- Broad exploration of post-processing surface modification for band-position tuning.
- High-throughput synthesis of appropriate electrocatalysts on α-$Fe_2O_3$ substrates compatible with electrolyte, and reactant/product properties.
- Heterostructure design with high efficiency of charge carrier separation.
- Iron oxide nanorod/microrod synthesis and control over growth structure.
- Single-sample slurry reactor for IQE measurement and quantitative $H_2$ analysis.

## FY 2008 Publications/Presentations

**1.** Y.-S. Hu, A. Kleiman-Shwarsctein, A. J. Forman, J.-N. Park, D. Hazen and E. W. McFarland, "Pt-doped α-$Fe_2O_3$ Thin Films Active for Photoelectrochemical Water Splitting", *Chem. Mater.* **2008**, *20*, 3803.

**2.** A. Kleiman-Shwarsctein, Y.-S. Hu, A. J. Forman, G. D. Stucky and E. W. McFarland, "Electrodeposition of α-$Fe_2O_3$ of doped with Mo and Cr and its application towards water splitting", *J. Phys. Chem. C.* (Accepted for publication).

**3.** E. W. McFarland, "*New Materials for PEC*", Invited talk, Danish Technical University, July 2007.

**4.** E. W. McFarland, "*Nanostructured Photoreactors*", Invited talk, Chalmers University, March 2008.

**5.** A. J. Forman, "*Multi-Component Nanostructured Semiconductors for Photoelectrocatalysis - Progress Towards Efficient and Stable Solar-to-Chemical Energy Conversion*", Oral presentation, Presented at Materials Research Society, March 2008.

**6.** A. Kleiman-Shwarsctein, "*Solar Hydrogen Production by Photo-oxidation of Water and Biomass with Hematite Nanorod Photoelectrocatalysts*" Poster, Presented at Materials Research Society, March 2008.

**7.** E. W. McFarland, "*PEC Hydrogen Production*", Invited tutorial, ECS Annual Meeting, June 2008.

**8.** E. W. McFarland. "*PEC Production of Fuels and Chemicals*", UCSB Symposium on Frontiers of Surface Science, June 2008.

## References

**1.** Khan S. U. M., A. J., J. Phys. Chem. B 1999, 103, 7184.

**2.** Bjorskten U, Moser J, Gratzel M, Chem. Mater, 6, 858.

**3.** Beermann N., Vayssieres L., Linquist E. S., Hagfeldt A., J. Electrochem. Soc. 2002, 147, 2456.

**4.** Ahmed S.M., Leduc J, Haller S.F., J. Phys. Chem. B 1988, 92, 6655.

**5.** Arutyunyan V.M., Arakelyan V.M., Sarkisyan A.G., Shakhnazaryan G.E., Stepanyan G.M., Turner J. A, Russ. J. Electrochem. 1998, 38, 854.

**6.** Vayssieres L., Beermann N., Lindquist S E, Hagfeldt A, Chem. Mater., 13,2, 2001, 233.

**7.** Kay A, Cesar I, and Grätzel M, Am. Chem. Soc., 128, 49, 2006, 15714.

**8.** Berry J. F., Greaves C., Helgason O., McManus J., J. Mater. Chem. 1999, 9, 223.

**9.** Prasad N. V, Srinivas K, Kumar S. G., J. A.R., Appl. Phys. A-Mater. 2001, 72, 341.

**10.** Aroutuaunian V.M., Arakelyan V.M., Shahnazaryan G.E., Stepanyan G.M., Turner J. A., Khaselev O, Int. J. Hydrogen Energ. 2002, 27, 33.